Progress in Physics of Applied Materials 6 (2026), Serial Number 10, 1 – 13

Semnan University

Progress in Physics of Applied Materials

journal homepage: https://ppam.semnan.ac.ir/

Structural and Magnetic Phase Transitions in $Cu_{1-3x}Zn_{2x}Mn_xFe_2O_4$ Ferrites

Ahmad Gholizadeh [a]*, Sakineh Hosseini [a]

[a] *School of Physics, Damghan University, Damghan, Iran*

ARTICLE INFO

Article history:
Received: 30 April 2025
Revised: 30 March 2025
Accepted: 6 May 2025
Published online: 15 August 2025

Keywords:
Spinel Ferrite;
Zn/Mn Co-Substitutions;
Structure Phase Transition;
Magnetic Properties.

ABSTRACT

Doping spinel ferrites with carefully selected dopants is a common approach to enhance the physical properties of the base ferrite. Zn/Mn co-substituted $CuFe_2O_4$, represented as $Cu_{1-3x}Zn_{2x}Mn_xFe_2O_4$, was prepared by the auto-combustion method. The primary goal was to study the effects of varying Zn/Mn levels on the structural, optical, and magnetic properties of $CuFe_2O_4$ spinel ferrites. As the Zn/Mn co-substitution level increased, a notable structural phase change from a tetragonal phase with $I4_1/amd$ space group to a cubic phase with $Fd\bar{3}m$ space group was observed. This finding was further validated through FTIR spectroscopy analysis. Interestingly, the bandgap energy of the co-substituted ferrites showed a clear dependence on the substitution levels, ranging from 1.68 eV to 1.98 eV. This variation in optical properties is a significant result, as it allows researchers to fine-tune the bandgap energy of these materials based on specific application requirements. Furthermore, the saturation magnetization of the co-substituted ferrites exhibited a considerable shift as the Zn/Mn levels increased. A hard-to-soft magnetic phase transition was observed, indicating a substantial change in the materials' magnetic behavior. This discovery highlights the potential to tailor the magnetic properties of $CuFe_2O_4$ spinel ferrites by carefully controlling the Zn/Mn co-substitution levels. Overall, the findings from this study demonstrate that Zn/Mn co-substitution is an effective technique to modify the properties of $CuFe_2O_4$ spinel ferrites.

1. Introduction

Due to varied properties, magnetic materials have long captivated researchers. Among these materials, spinel structures have stood out for their desirable characteristics, such as high adsorption capacity, chemical stability, and diverse functionalities. These versatile properties have propelled their widespread applications in fields ranging from data storage and recording to drug delivery systems and microwave absorption. The promising future of spinel ferrites extends far beyond these initial applications [1-3]. Their magnetic, optical, and catalytic properties are being harnessed for photocatalysis, sensing devices, optoelectronics, and more, propelling them to the forefront of emerging technologies. This diverse functionality makes spinel ferrites an exciting area of research for scientists, engineers, and inventors seeking to harness their potential for the next generation of technological advancements [4-7].

Spinel ferrites exhibit intriguing properties due to their unique crystal structure and general chemical formula, MFe_2O_4. In this formula, M represents a divalent cation, which occupies the tetrahedral (A) crystallographic sites within the spinel lattice. These cations play a determining role for the physical properties of the material. The cation selection profoundly affects the electronic structure, magnetic behavior, and other properties, such as band gap and coercivity. This makes spinel ferrites highly versatile, and with careful synthesis methods like sol-gel, their potential can be tailored for various applications in fields like data storage, optical sensing, and catalysis. With a deeper understanding of the role of cations in spinel ferrites, research has turned to modifying their properties through the addition of foreign ions. This technique, known

* Corresponding author. Tel.: +98-912-0816781
E-mail address: gholizadeh@du.ac.ir

Cite this article as:
Gholizadeh A, and Hosseini S., 2026. Structural and magnetic phase transitions in $Cu_{1-3x}Zn_{2x}Mn_xFe_2O_4$ ferrites. *Progress in Physics of Applied Materials*, *6*(1), pp.1-13.DOI: **10.22075/PPAM.2025.37277.1141**

as co-doping, is emerging as an effective strategy for fine-tuning the properties of ferrites for specialized applications [8,9]. The co-doping of spinel ferrites has opened the door for further customization of these materials to meet specific requirements. By strategically selecting and controlling the amount of co-doped ions, it is possible to achieve enhanced performance in a range of technological applications [10-13].

Multiple studies have explored the preparation and modification of spinel ferrites to enhance their properties for various applications. Ferreira et al. [14] used a proteic sol-gel auto-combustion method to synthesize MFe_2O_4 (M = Ni, Co, Cu) spinel ferrites, demonstrating the effectiveness of this method in obtaining ferrite materials with controlled physical properties. Rietveld refinement confirmed the pure phase cubic structure of the ferrites, which also exhibited ferromagnetic behavior. This research underlines the potential of sol-gel methods for synthesizing ferrite materials with desirable properties. In another study, Vinnik et al. [15] studied the effects of Co/Zn co-substitution on the physical properties of $NiFe_2O_4$ ferrites. XRD analysis validated the formation of a pure-phase structure with a complex relationship between Co content and saturation magnetization, revealing a non-linear correlation. Furthermore, an increase in remnant magnetization and coercivity was noted as Co content increased, indicating the intricate role of Co substitution in shaping the magnetic behavior of these magnetic materials. Structural characterization of Mn-doped Co/Zn spinel ferrites through XRD and FTIR showed the cubic symmetry of the spinel structure [16]. The ferrites exhibited soft ferromagnetic behavior, as determined by magnetic measurements using a VSM. This finding emphasizes the efficacy of the sol-gel method in synthesizing spinel ferrites with desirable structural and magnetic properties. XRD analysis of Zn-substituted $MnFe_2O_4$ spinels confirmed the formation of a cubic structure of the samples and showed that increasing Zn concentration led to an increase in particle size [17]. This study demonstrates the potential of chemical substitution in modifying the properties of spinel materials, opening up new avenues for developing advanced magnetic materials. SEM and TEM analyses further validated the nano-sized nature of the materials, providing valuable insights into the structural and morphological changes caused by Zn substitution. These findings suggest that Zn substitution can notably influence the physical properties of $MnFe_2O_4$ spinels, presenting a promising avenue for material optimization. Several studies have focused on the effects of chemical substitution on the properties of spinel ferrites, highlighting the potential for tailoring the spinel materials for various applications. Shertyuk et al. [18] reported the formation of a single-phase Co-substituted Ni/Zn spinel ferrites synthesized through a solid-state reaction method. The results demonstrated an enhancement in saturation magnetization, remanent magnetization, and coercivity with increasing Co substitution, attributed to the larger magnetic moment of Co^{2+} compared to Ni^{2+}. This finding underscores the role of Co doping in modulating the physical properties of ferrites. In a separate study, Nasr et al. [19] reported that Rietveld refinement of XRD pattern of Co/Cd spinel ferrites confirmed the successful formation of a single-phase structure, demonstrating the effective incorporation of Co and Cd into the spinel lattice. FTIR analysis revealed two absorption bonds associated with the spinel structure. Vibrating sample magnetometer (VSM) measurements showed an increase in both saturation magnetization and coercive field with higher Co content, indicating an improvement in the ferromagnetic ordering of the ferrites. This result showed the potential of Co substitution in tuning the magnetic properties of spinels. Dojcinovic et al. [20] explored that XRD and FTIR analyses of Mg/Co spinel ferrites validated the formation of a pure spinel structure. The magnetic properties of the samples were significantly enhanced upon substituting Mg^{2+} ions with Co^{2+}, demonstrating the impact of co-substitution on the overall magnetic behavior of these materials. Additionally, a decrease in bandgap energy from 2.09 eV value for $MgFe_2O_4$ spinel ferrite to 1.42 eV value for $CoFe_2O_4$ ferrite was observed, indicating that co-substitution can also influence the electronic properties of ferrites. Collectively, these studies emphasize the importance of chemical substitution in modulating the structural, magnetic, and electronic properties of spinel ferrites. By carefully controlling the type and concentration of substituting elements, researchers can tailor these materials for technological applications, where specific magnetic properties are required.

The synthesis and characterization of Zn/Mn co-substituted $CuFe_2O_4$ ferrites have been a focus in recent research, aiming to bridge the knowledge gap on the properties of these novel materials. While phase transitions in other Zn/Mn co-substituted ferrite systems, such as Ni-Zn-Mn or Co-Zn-Mn, have been previously reported [21-24], our work specifically focuses on the $CuFe_2O_4$-based system. To the best of our knowledge, the tetragonal-to-cubic transition induced by Zn/Mn co-substitution in $CuFe_2O_4$ ferrites has not been previously documented in the literature. This work employs the sol-gel citrate-nitrate method to synthesize a series of Zn/Mn co-substituted $CuFe_2O_4$ spinel ferrites with varying concentrations of substituting ions. The introduction of Zn^{2+} and Mn^{2+} ions, having different ionic radii than the native Cu^{2+} and Fe^{3+} ions in $CuFe_2O_4$, leads to structural perturbations that significantly change the overall properties of the samples. To better understand the effects of Zn^{2+} and Mn^{2+} co-substitution on $CuFe_2O_4$ nanoparticles, the structural, morphological, magnetic, and optical properties of the Zn/Mn co-substituted samples were extensively studied. By analyzing previous research on the effects of co-substitution in spinel ferrites, this work explores how the incorporation of Zn and Mn influences various properties of $CuFe_2O_4$ nanoparticles. The subsequent sections provide a good discussion of the properties of Zn/Mn co-substituted $CuFe_2O_4$ nanoparticles. These discussions are guided by the findings of earlier studies, focusing on the structural perturbations caused by the substituting cations and their effects on the overall properties of the samples.

The goal is to understand the potential applications of $Cu_{1-3x}Zn_{2x}Mn_xFe_2O_4$ in different fields, including magnetic materials, electronics, and energy storage.

The specific stoichiometry of $Cu_{1-3x}Zn_{2x}Mn_xFe_2O_4$ was selected based on a combination of factors. Firstly, the coefficients 1-3x, 2x, and x were chosen to maintain the overall charge neutrality of the spinel structure, where the total positive charge contributed by Cu^{2+}, Zn^{2+}, Mn^{2+}, and Fe^{3+} ions should equal the total negative charge contributed by oxygen ions. By varying the x value, we aimed to introduce different amounts of Zn and Mn dopants while maintaining charge balance within the system. Secondly, the ionic radii of Cu^{2+}, Zn^{2+}, Mn^{2+}, and Fe^{3+} ions are relatively close to each other, facilitating the successful incorporation of Zn and Mn dopants into the $CuFe_2O_4$ lattice without significant structural distortion. The ionic radii matching between the dopants and host cations is critical for obtaining stable and well-defined materials. Finally, the stoichiometry was selected to tailor the magnetic properties of $CuFe_2O_4$ ferrites through the incorporation of Zn and Mn dopants. The magnetic moment optimization in our study aimed to achieve a hard to soft magnetic phase transition by fine-tuning the Zn/Mn substitution levels, as both Zn^{2+} and Mn^{2+} ions have different magnetic moments compared to Cu^{2+} and Fe^{3+} ions.

Our work on $Cu_{1-3x}Zn_{2x}Mn_xFe_2O_4$ ferrites contributes significantly to the existing body of knowledge in several ways: (1) Structural phase transition: Our findings reveal a notable structural phase transition from a tetragonal phase to a cubic phase as the Zn/Mn co-substitution level increases. This observation adds to the understanding of the effects of dopant concentration on the structural properties of spinel ferrites. (2) Optical properties: We demonstrate that varying the Zn/Mn substitution levels leads to a clear dependence of the bandgap energy on the dopant concentration, allowing for the fine-tuning of optical properties based on application requirements. (3) Magnetic phase transition: Our study highlights a substantial change in the magnetic behavior of $CuFe_2O_4$ ferrites induced by the introduction of Zn and Mn dopants. The observation of a hard to soft magnetic phase transition with increasing Zn/Mn substitution levels contributes to the understanding of how to tailor the magnetic properties of spinel ferrites through co-substitution.

By examining the properties of these novel materials in detail, this research sheds light on how Zn/Mn co-substitution can be utilized to modify and optimize the properties of $CuFe_2O_4$ nanoparticles. This understanding is crucial for the synthesis of tailored materials for selected applications, ultimately contributing to advancements in various industries.

2. Experimental

2.1. Synthesis of the Samples

The preparation of the $Cu_{1-3x}Zn_{2x}Mn_xFe_2O_4$ was carried out using a sol-gel citrate-nitrate method according to Refs. [25,26]. Specifically, $Cu(NO_3)_2.3H_2O$, $Mn(NO_3)_2.4H_2O$, $Zn(NO_3)_2.4H_2O$, and $Fe(NO_3)_3.9H_2O$, obtained from Sigma-Aldrich with a chemical purity of over 99%, were employed as starting reagents for the synthesis process. The synthesis of $Cu_{1-3x}Zn_{2x}Mn_xFe_2O_4$ nanoparticles was commenced by preparing a homogeneous solution of the precursors in the deionized water, stirred by a magnetic stirrer. The solution was then combined with a citric acid solution in a molar ratio of 1:1, thus creating a mixture of the desired composition. The mixture was stirred until a uniform brownish color was achieved, then transferred to a hot water bath and heated to a temperature of 80 °C until it developed a gel-like consistency. The resulting gel was then placed in an oven at a temperature of 200 °C for 12 hours to allow residual solvent evaporation and further drying of the resulted material. Following this, the dried gel was calcined at a temperature of 900 °C for 3 hours in a furnace, which triggered the crystallization process, resulting in the formation of $Cu_{1-3x}Zn_{2x}Mn_xFe_2O_4$ nanoparticles. Once the nanoparticles were successfully formed, the samples were collected, and investigated to a range of characterization methods to examine their physical properties.

The selection of a calcination temperature of 900°C was based on a thorough review of existing literature and preliminary experiments conducted in our lab. Our experiments demonstrated that a calcination temperature of 900°C produced well-crystallized $Cu_{1-3x}Zn_{2x}Mn_xFe_2O_4$ ferrites with minimal impurity phases. Additionally, our choice of calcination temperature was guided by the need to achieve a balance between the formation of the desired spinel phase and the prevention of excessive particle growth and agglomeration. A higher calcination temperature may lead to increased particle size, while a lower temperature may result in incomplete crystallization and the presence of impurity phases.

2.2. Characterizations

To obtain a detailed properties of Zn/Mn co-substituted $CuFe_2O_4$ nanoparticles, several advanced characterization techniques were employed. These techniques provided comprehensive insights into the structural, morphological, optical, and magnetic properties of the synthesized materials. XRD patterns of $Cu_{1-3x}Zn_{2x}Mn_xFe_2O_4$ were recorded using a D8 Advance diffractometer (Bruker-AXS, Cu-Kα anode). This technique allowed for the analysis of the structure and phase composition of the nanoparticles. The surface morphology of the Zn/Mn co-substituted $CuFe_2O_4$ nanoparticles was examined using a field-emission scanning electron microscope (FE-SEM, TESCAN MIRA3). This high-resolution imaging technique provided detailed information on the particle size, and surface texture of the synthesized materials. In addition, energy-dispersive X-ray (EDX) analysis, integrated with the FE-SEM system, was employed to determine the elemental composition of the nanoparticles. Ultraviolet-visible (UV-Vis) absorbance spectra of the Zn/Mn co-substituted $CuFe_2O_4$ nanoparticles were obtained in the 400-1100 nm wavelength range using a UNICO-4802 UV-Vis Spectrophotometer. This technique allowed for the analysis of bandgap energy of the prepared samples. Finally, the magnetic properties of the Zn/Mn co-substituted $CuFe_2O_4$ nanoparticles were investigated by recording hysteresis loops with a magnetic field of 15 kOe, using a VSM-7300 vibrating sample magnetometer at room temperature, which provided coercivity, saturation magnetization, and remanent magnetization. A combination of state-of-the-art characterization

techniques was employed to obtain a comprehensive understanding of the microstructural, optical, and magnetic properties of Zn/Mn co-substituted $CuFe_2O_4$ nanoparticles. These techniques provided valuable insights into the effects of Zn/Mn co-substitution on the properties of $CuFe_2O_4$ nanoparticles, paving the way for further optimization of these samples.

3. Results and Discussion

3.1. Structural Analysis

XRD analysis of $Cu_{1-3x}Zn_{2x}Mn_xFe_2O_4$ revealed substantial changes in the crystal structure as the Zn/Mn co-substitution level increased. As seen in Fig. 1, the XRD patterns of the samples exhibited a gradual tetragonal-to-cubic transition with increasing Zn/Mn co-substitution. Table 1 shows the crystallographic findings of the samples. For the pristine $CuFe_2O_4$ sample (x = 0.00), the XRD pattern matched the tetragonal lattice with I41/amd space group, corresponding to the ICDD card No. 00-034-0425 [27,28]. This transition began at x = 0.03 and was completed at x = 0.15, as evidenced by the emergence of a cubic lattice with $Fd\bar{3}m$ space group in the XRD pattern of x = 0.12 sample and x = 0.15 sample (ICDD card number 01-077-0010) [29,30]. The observed structural shift from tetragonal-to-cubic phase can be attributed to the changes in the structural characteristics of the samples due to the co-substitution of Zn^{2+} and Mn^{2+} ions for Cu^{2+} and Fe^{3+} ions, respectively.

The difference in the ionic radii and electronic configurations between the substituting and native ions likely disrupts the spinel lattice, leading to a modification in the crystal phase. Overall, the XRD analysis provides valuable insights into the structural evolution of $CuFe_2O_4$ spinel ferrites upon the Zn/Mn co-substitution.

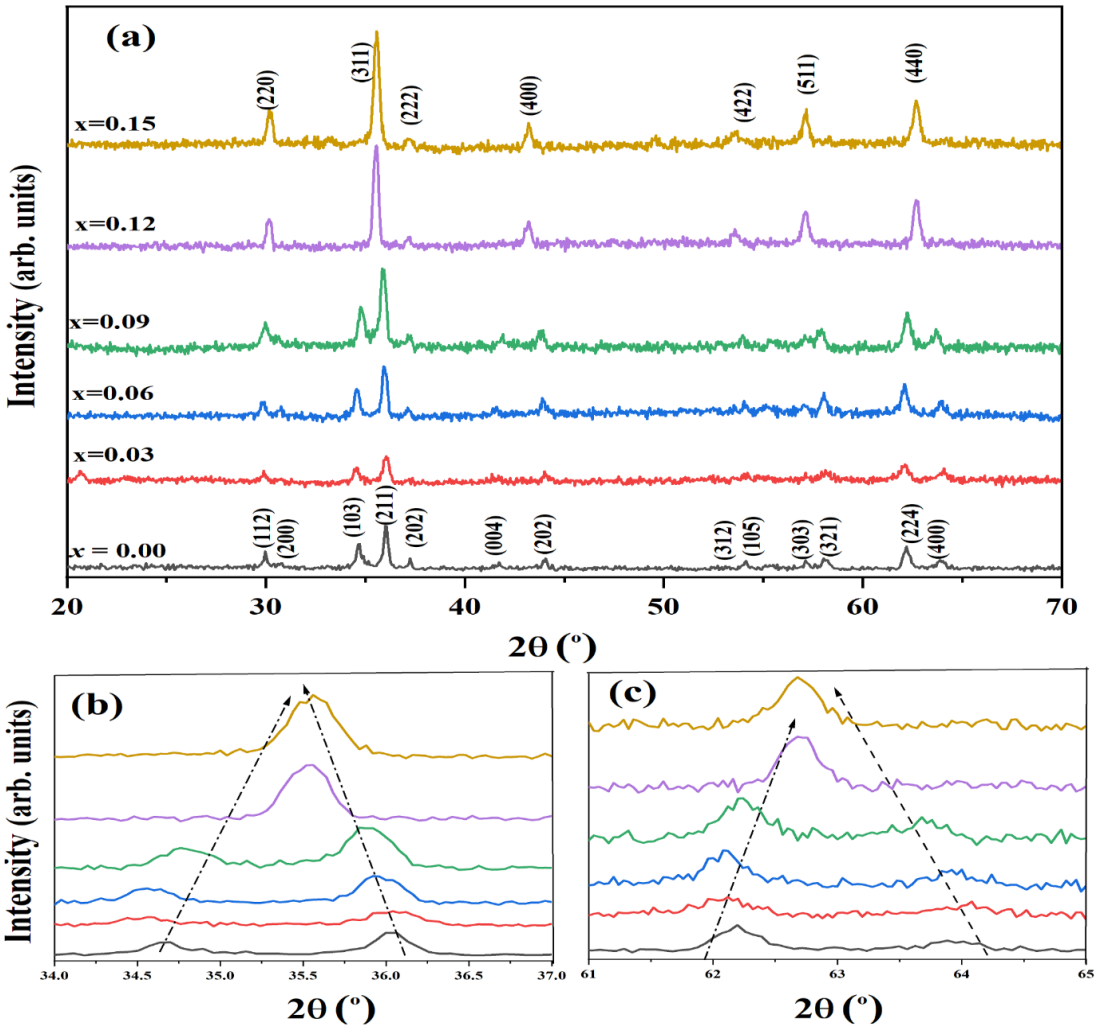

Fig. 1. (a) XRD pattern of the $Cu_{1-3x}Zn_{2x}Mn_xFe_2O_4$ spinel ferrites, (b), and (c) merging the XRD peaks indicates tetragonal-to-cubic phase transition.

This transformation from tetragonal to cubic phase with increasing the Zn/Mn co-substitution levels highlights the significant chemical impact of co-substitutions on the crystallographic lattice of these materials, which can further influence their physical properties and potential applications.

Table 1. Crystallographic findings of the $Cu_{1-3x}Zn_{2x}Mn_xFe_2O_4$ spinel ferrite nanoparticles

2θ (°)	FWHM (°)	D_{Sch} (nm)	d_{hkl} (Å)	Identification with d_{hkl} (Å)	(hkl)	structure
$CuFe_2O_4$ (x = 0.00)						
35.68	0.5580	15.0	2.50	2.50	211	Tetragonal
$Cu_{0.91}Zn_{0.06}Mn_{0.03}Fe_2O_4$ (x = 0.03)						
36.0	0.3303	25.3	2.49	2.50	211	Tetragonal
				2.52	311	Cubic
$Cu_{0.82}Zn_{0.12}Mn_{0.06}Fe_2O_4$ (x = 0.06)						
35.92	0.2464	33.9	2.50	2.50	211	Tetragonal
				2.52	311	Cubic
$Cu_{0.73}Zn_{0.18}Mn_{0.09}Fe_2O_4$ (x = 0.09)						
35.86	0.2972	28.1	2.50	2.50	211	Tetragonal
				2.52	311	Cubic
$Cu_{0.64}Zn_{0.24}Mn_{0.12}Fe_2O_4$ (x = 0.12)						
35.52	0.2963	28.2	2.52	2.50	211	Tetragonal
				2.52	311	Cubic
$Cu_{0.55}Zn_{0.3}Mn_{0.015}Fe_2O_4$ (x = 0.15)						
35.49	0.2444	34.2	2.52	2.52	311	Cubic

The lattice parameters for the samples were determined using Eq. (1) for the tetragonal spinel phase, and Eq. (2) was used for those with a cubic spinel phase [28]:

$$\frac{4\,sin^2\,\theta}{\lambda^2} = \frac{h^2+k^2}{a^2} + \frac{l^2}{c^2} \quad (1)$$

$$\frac{4\,sin^2\,\theta}{\lambda^2} = \frac{h^2+k^2+l^2}{a^2} \quad (2)$$

The lattice parameters, denoted as c and a, are calculated using the diffraction angle θ from X-ray peaks, with the wavelength λ=1.54 Å. For the cubic structure, lattice parameters are derived from the (311) peak using the selected Miller indices. For the tetragonal structure, lattice parameters are calculated using the (211) and (224) peaks. The variation of lattice parameters with substitution level x is provided in Table 2.

Table 2. Geometric parameters of the $Cu_{1-3x}Zn_{2x}Co_xFe_2O_4$ ferrite

Sample	Lattice parameters			*c/a*	*V*
	a (Å)	***a**** (Å)	***c*** (Å)		**(Å³)**
x = 0.00	5.822	8.233	8.671	1.489	558.05
x = 0.03	5.836	8.254	8.655	1.483	562.33
x = 0.06	5.848	8.271	8.631	1.476	565.81
x = 0.09	5.877	8.312	8.577	1.459	574.27
x = 0.12	---	8.309	---	---	573.65
x = 0.15	---	8.305	---	---	572.82

It is well-established that the tetragonal lattice of $CuFe_2O_4$ can be viewed as a non-standard centrosymmetric structure (space group $F4_1/ddm$) with a c/a ratio of 1.6, consisting of 8 formula units of $CuFe_2O_4$ [28-30]. Typically, the tetragonal-to-cubic transition is understood as a compression or elongation along one of the FCC axes. Consequently, the structure adopts a non-standard centrosymmetric tetragonal form (space group $F4_1/ddm$), where the lattice parameters are given by $a^* = a_{tetr}\sqrt{2}$ and $c^* = c$ corresponding to the $F4_1/ddm$ space group [28-30]. As indicated in Table 2, an increase in Zn/Co substitution leads to a corresponding increase in $a*$. $CuFe_2O_4$ with a tetragonal spinel structure exhibits an inverse structure with δ approaching 1, where all Cu^{2+} ions occupy the B site, and Fe^{3+} ions are equally distributed between the A and B sites [28-30]. $CuFe_2O_4$ is a fully inverse spinel, where half of the iron cations, along with all Cu^{2+} cations, occupy the B site, while the remaining iron cations occupy the A site, resulting in a structure like $(Fe^{+3})_A\ [Fe^{+3}Cu^{+2}]_BO_4^{-2}$. The presence of Cu^{2+} cations at the B site induces Jahn-Teller distortion, which leads to the formation of a tetragonal spinel structure with the $I4_1/amd$ space group [28-30]. However, under certain synthesis conditions and annealing temperatures, a mixed-spin $CuFe_2O_4$ structure with cubic symmetry (space group $Fd\bar{3}m$) can be achieved.

3.2. FTIR Analysis

FTIR spectra of $Cu_{1-3x}Zn_{2x}Mn_xFe_2O_4$ in the range of 400 to 4000 cm^{-1} revealed distinct absorption bonds that shed light on the bond length and angle changes induced by Zn/Mn co-substitution. As shown in Figure 2, the FTIR spectra exhibited two characteristic absorption bonds related to the vibrations of the A- and B-sites in the spinel lattice [31,32].

The higher-frequency bond ($\bar{\nu}_t$), observed within the 608-618 cm^{-1} range, corresponds to the vibration of the A site (M_{tetra}-O). As seen in Table 3, an increase in Zn/Mn co-substitution resulted in a red shift of this bond, suggesting a change in the vibration of the A site. The lower-frequency bond ($\bar{\nu}_o$), detected in the 474-492 cm^{-1} range, is related to the B-site vibration (M_{octa}-O). As the co-substitution level increased, this bond exhibited a red shift, implying a change in the B-site vibration (see Table 3). These shifts in the absorption bonds can be attributed to modifications in the bond length and angle at the tetragonal and octahedral sites as a result of Zn/Mn co-substitution [33]. Specifically, the A site undergoes compression, while the B site experiences elongation, which can be ascribed to changes in the lattice parameters within the spinel lattice. The observed tetragonal-to-cubic structural transition upon increasing Zn/Mn co-substitution appears to be linked to the alterations in the bond lengths at the A and B sites. The distinct ionic radii and electronic configurations of the substituted Zn^{2+} and Mn^{2+} ions contribute to the compression of the A site and the elongation of the B site, ultimately driving the phase transition in the material's structure.

In conclusion, the FTIR analysis indicates valuable results into the structural evolution of Zn/Mn co-substituted $CuFe_2O_4$ spinel ferrites. The changes in the A and B site vibrations observed in the absorption bonds reveals that the tetragonal-to-cubic structural transition is associated with modifications in the lattice parameters due to the co-substitution of Zn^{2+} and Mn^{2+} ions.

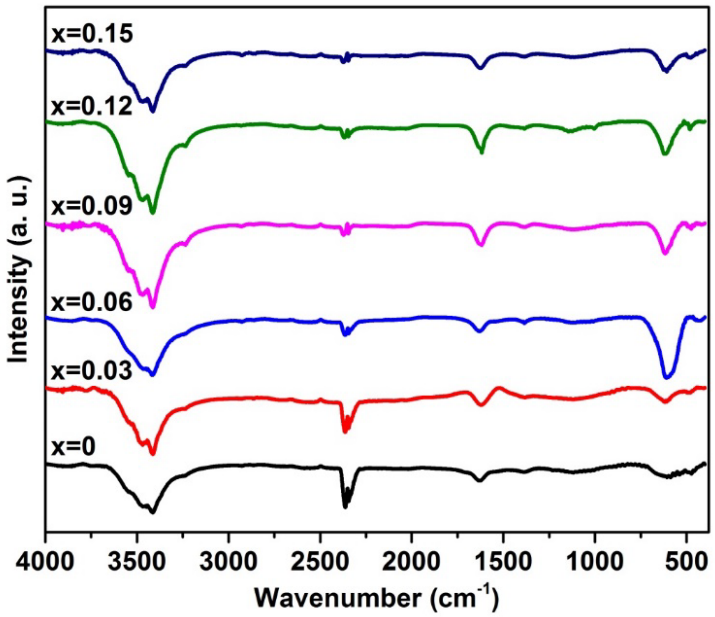

Fig. 2. FTIR absorption spectrum of the $Cu_{1-3x}Zn_{2x}Mn_xFe_2O_4$ spinel ferrite

Table 3. Positions of absorption peaks appeared in the FTIR spectra of $Cu_{1-3x}Zn_{2x}Mn_xFe_2O_4$ spinel ferrites

Sample	$\bar{\nu}_o$(cm^{-1})	$\bar{\nu}_t$ (cm^{-1})
***x* = 0.00**	602	470
***x* = 0.03**	606	472
***x* = 0.06**	610	475
***x* = 0.09**	613	480
***x* = 0.12**	615	486
***x* = 0.15**	615	488

3.3. Morphological Properties

The morphology of $Cu_{1-3x}Zn_{2x}Mn_xFe_2O_4$ (x = 0.00, 0.03, 0.09, and 0.15) was analyzed via FESEM imaging shown in Figure 3, revealing an interesting increase in particle size upon co-substitution. As can be seen, Zn/Mn substitution causes larger aggregates and the size of particles is gradually increased. Size distribution histograms of samples are shown in Figure 4. According to these histograms, the mean grain size of the $CuFe_2O_4$, $Cu_{0.91}Zn_{0.06}Mn_{0.03}Fe_2O_4$, $Cu_{0.73}Zn_{0.18}Mn_{0.09}Fe_2O_4$, and $Cu_{0.55}Zn_{0.30}Mn_{0.15}Fe_2O_4$ samples were 190.65 nm, 986.79 nm, 927.62 nm, and 906.65 nm, respectively. Size distribution histograms are fitted by using a log-normal function. It is clear that the obtained values confirm our previous observations from FESEM images. The possible contributing factors for this observed phenomenon are as follows: The particle size increase observed in Zn/Mn co-substituted $CuFe_2O_4$ spinel ferrites are likely influenced by factors beyond the similar ionic radii of Mn^{3+}, Zn^{2+}, and Cu^{2+} ions [34]. While ionic radii can play a role in determining particle size, the lack of a direct correlation suggests that other factors may be at play. One such factor could be the variation in electronegativity value between the guest (Zn and Mn) and host cations, which can lead to a decrease in bonding strength. Consequently, this reduction in bonding strength can increase the value of particle size of the ferrites. Additionally, the co-substitution process can alter the growth dynamics of the nanoparticles, potentially promoting formation of larger particles through mechanisms such as Ostwald ripening or particle aggregation [35,36].

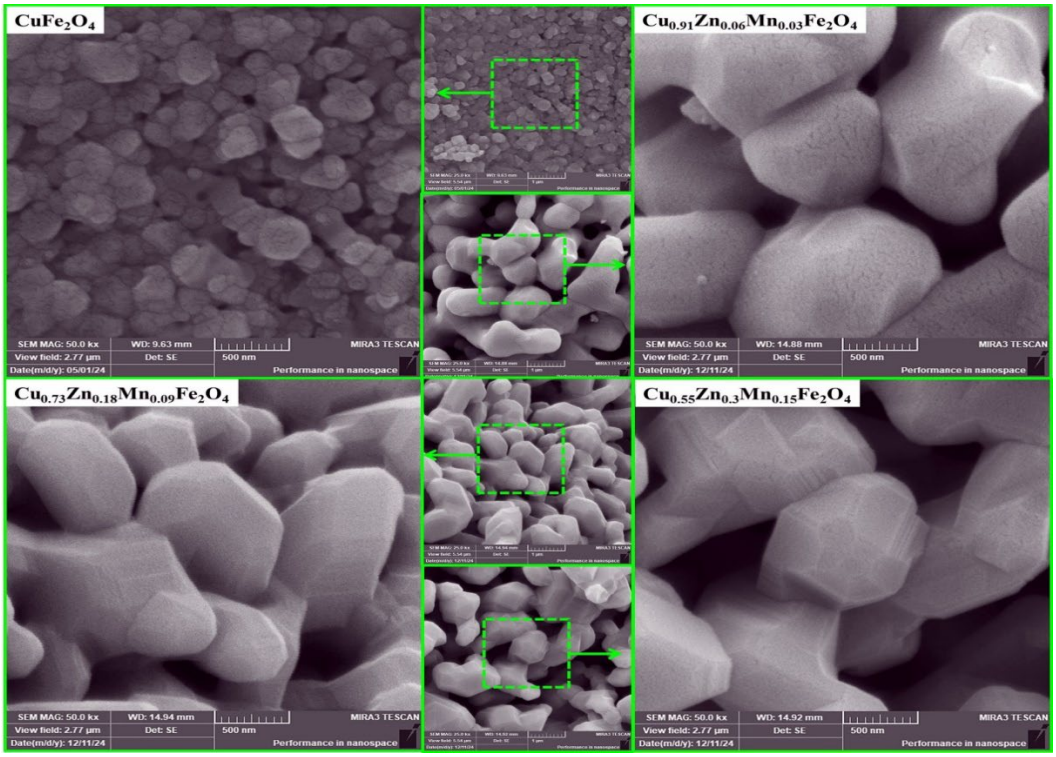

Fig. 3. FESEM images of $Cu_{1-3x}Zn_{2x}Mn_xFe_2O_4$ samples

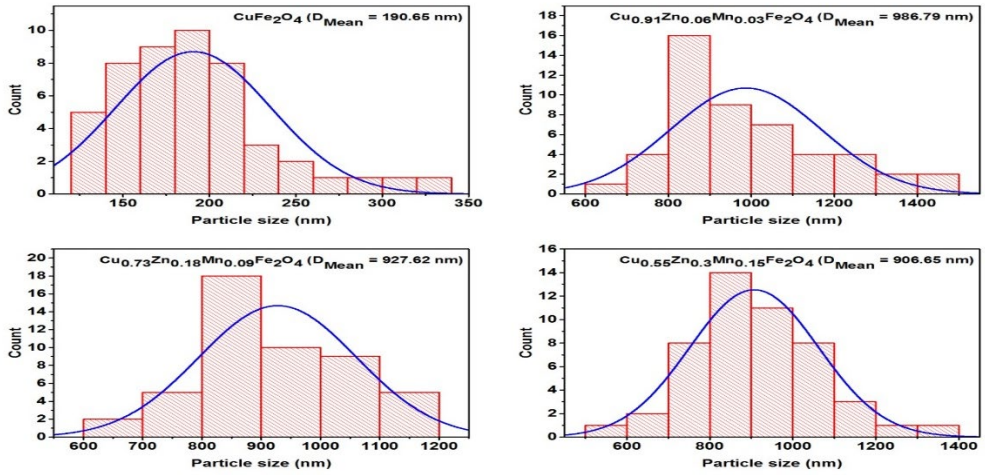

Fig. 4. Size distribution histograms of the $Cu_{1-3x}Zn_{2x}Mn_xFe_2O_4$ (x = 0, 0.03, 0.09, and 0.15) spinel ferrite nanoparticles

Ostwald ripening involves the dissolution of smaller particles and the redeposition of their material onto larger particles, while particle aggregation refers to the clustering of particles due to attractive forces. These processes can help to the increase observed in the particle size in the Zn/Mn co-substituted $CuFe_2O_4$. Energy-dispersive X-ray (EDX) analysis of the $Cu_{1-3x}Zn_{2x}Mn_xFe_2O_4$ (x = 0.00, 0.03, 0.09, and 0.15) provide concrete evidence of the successful incorporation of these elements into the spinel lattice (see Figure 5). The EDX results revealed the presence of Cu, Zn, Mn, Fe, and O in the synthesized nanoparticles, offering valuable insights into their elemental composition and stoichiometry.

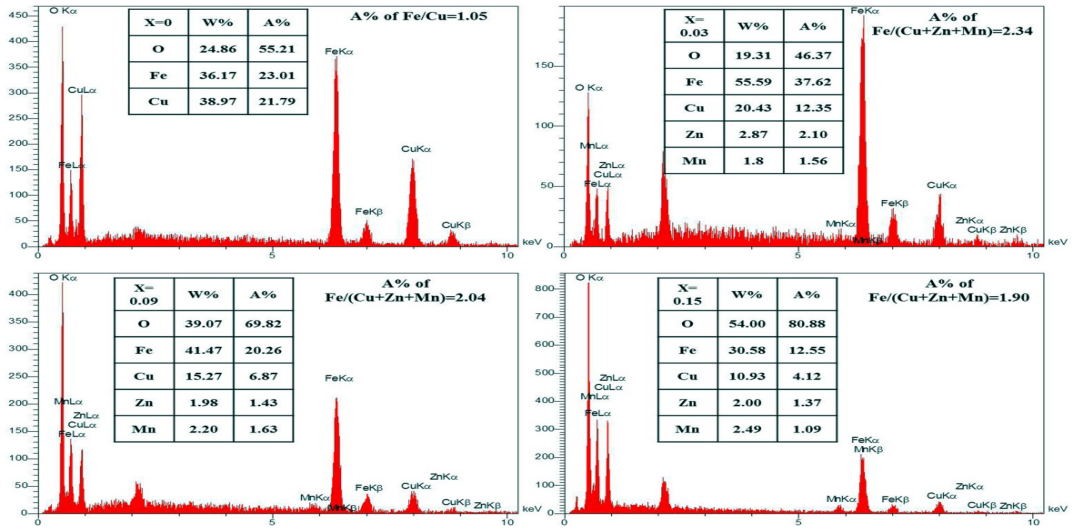

Fig. 5. EDS analysis of $Cu_{1-3x}Zn_{2x}Mn_xFe_2O_4$ samples

The close agreement between the weight and atomic percentages obtained from EDX analysis and the theoretical values supports the effectiveness of the chosen synthesis approach and the successful incorporation of Zn and Mn into the spinel structure. This indicates that the citrate-nitrate method can be employed to produce tailor-made Zn/Mn co-substituted $CuFe_2O_4$ nanoparticles with controllable elemental compositions for various applications.

3.4. Optical Properties

The effect of Zn/Mn co-substitution on the band gap of $Cu_{1-3x}Zn_{2x}Mn_xFe_2O_4$ powders was studied using the Tauc model, which confirmed a significant decrease in the band gap energy with increasing Zn/Mn and decreasing Cu contents. To calculate the band gap of the $Cu_{1-3x}Zn_{2x}Mn_xFe_2O_4$, the following relation between the absorption coefficient (α) and the photon energy (hν) was utilized [37,38]:

$$(\alpha h\nu)^2 = A(h\nu - E_g) \quad (3)$$

In this equation, A represents a constant, Eg denotes the bandgap energy, and n is an exponent that varies depending on the type of electronic transition involved (n = 1/2 for direct and n = 2 for indirect transition). The analysis of the bandgap energy revealed that the

$Cu_{0.91}Zn_{0.06}Mn_{0.03}Fe_2O_4$ sample exhibited the highest Eg value of 1.98 eV, while the $Cu_{0.55}Zn_{0.3}Mn_{0.15}Fe_2O_4$ sample displayed the lowest band gap of 1.68 eV (Figure 6 and Table 4). A decreasing trend in the band gap was observed with the Zn/Mn co-substitution, suggesting a reduction in the ionic bond strength due to changes in the electronic structure of the nanoparticles.

Table 4. Bandgap energy values of $Cu_{1-3x}Zn_{2x}Mn_xFe_2O_4$ spinel ferrites

Sample	E_g (eV)
x = 0.03	1.98
x = 0.06	1.87
x = 0.09	1.82
x = 0.12	1.71
x = 0.15	1.68

The decrease in bandgap energy could be advantageous for certain applications, such as in photocatalysis or solar energy conversion, where lower bandgap materials can utilize a broader range of the solar spectrum. Additionally, these findings provide valuable insights into the tuning of electronic properties of spinel ferrites through chemical co-substitution, enabling the development of ferrite materials with tailored electronic characteristics for specific applications.

3.5. Magnetic Properties

An examination of the magnetic properties of $Cu_{1-3x}Zn_{2x}Mn_xFe_2O_4$ revealed that increasing the degree of co-substitution significantly impacted the saturation magnetization (M_s) and coercive field (H_c) of the studied materials (see Figure 7). The values of coercive field (H_c), remanent magnetization (M_r), and saturation magnetization (M_s) for all samples were extracted from the hysteresis loops and are listed in Table 5.

It is observed that with an increase in Zn/Mn co-substitution, the total saturation magnetization of the samples increases (from 18.62 emu/g for x = 0 to 33.95 emu/g for x = 0.15). With increasing the Zn/Mn co-substitution, a hard-to-soft magnetic phase transition was observed in such a way that a sharp decrease in the coercive field of the samples is observed (from 1318.88 Oe for x = 0 to 35.86 Oe for x = 0.15), while the saturation magnetization increases.

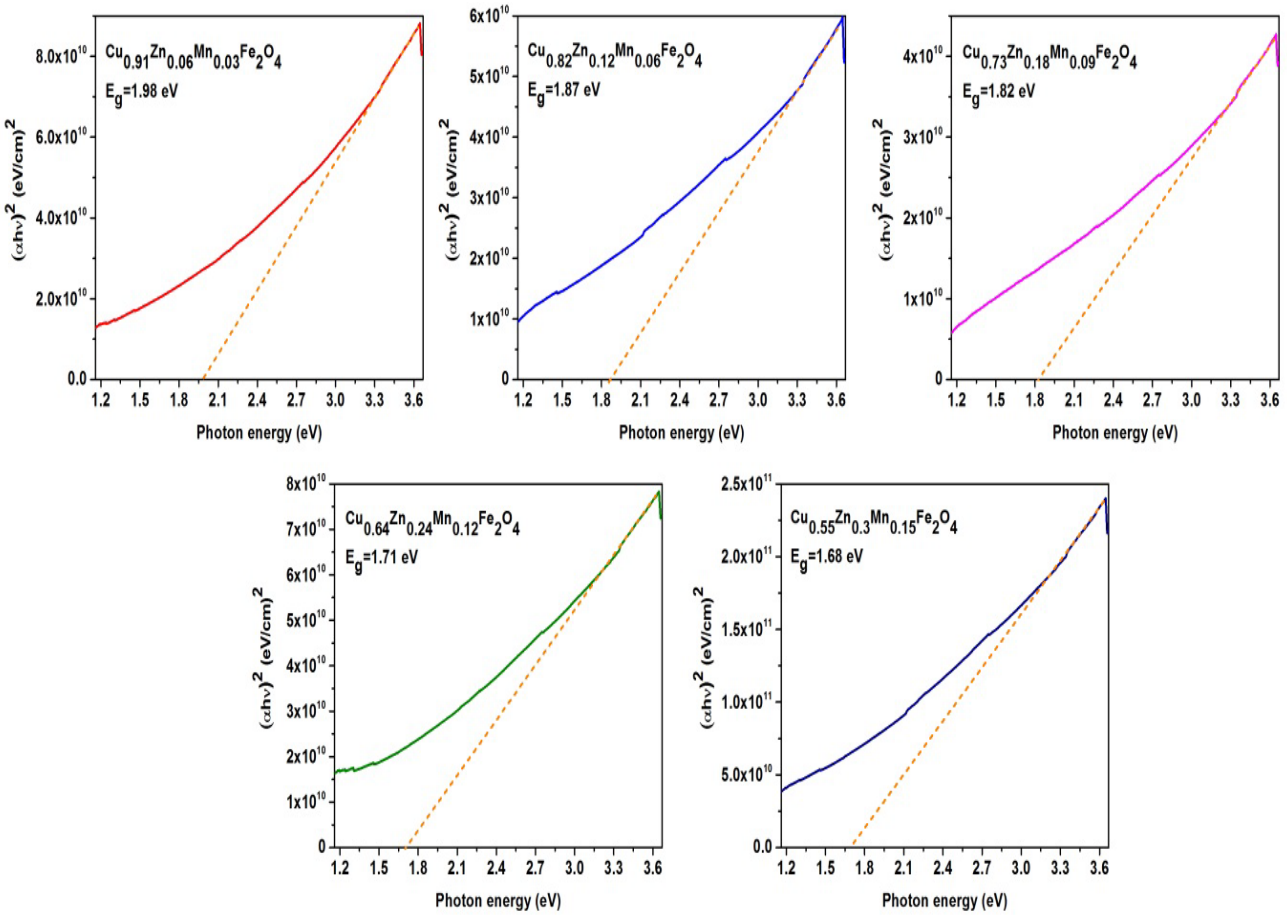

Fig. 6. Optical band gap energy of the $Cu_{1-3x}Zn_{2x}Mn_xFe_2O_4$ spinel ferrite

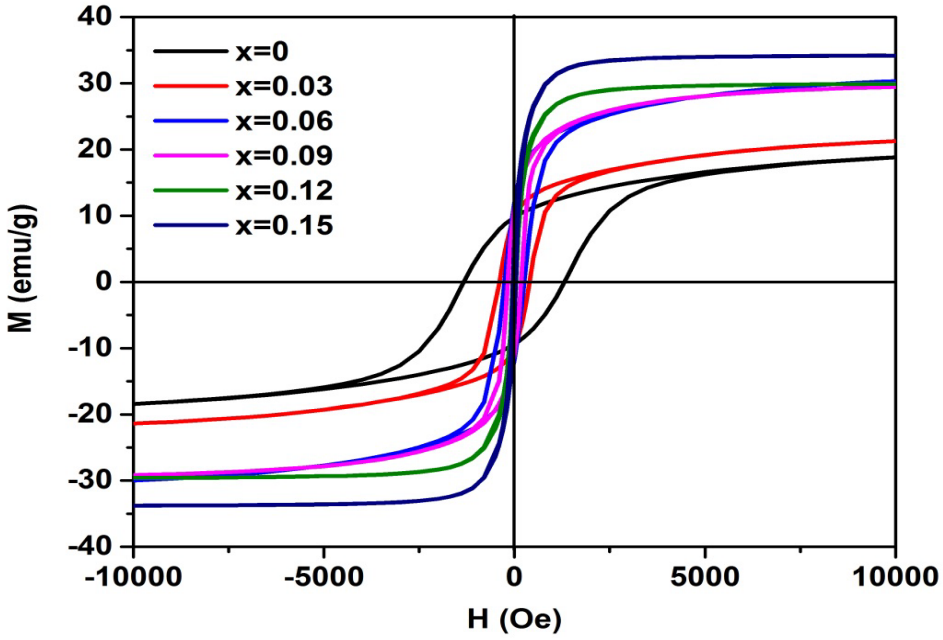

Fig. 7. Hysteresis loops of the $Cu_{1-3x}Zn_{2x}Mn_xFe_2O_4$ spinel ferrite

Table 5. Values of magnetic parameters for $Cu_{1-3x}Zn_{2x}Mn_xFe_2O_4$ spinel ferrites

Sample	M_s(emu/g)	M_r (emu/g)	H_c (Oe)	M_r / M_s
x = 0.00	18.62	9.57	1318.88	0.51
x = 0.03	21.30	9.79	392.98	0.45
x = 0.06	30.14	11.90	257.49	0.39
x = 0.09	29.30	11.11	174.26	0.37
x = 0.12	29.73	5.33	41.4	0.17
x = 0.15	33.95	5.96	35.86	0.17

Two primary factors contribute to these observed changes in magnetic properties: enhanced particle size and modified cation redistribution within the spinel lattice. The increase in particle size resulting from Zn/Mn co-substitution can directly impact the magnetic properties, as larger particles can exhibit higher M_s values due to stronger magnetic interactions among the particles. Additionally, the redistribution of cations within the crystal lattice induced by Zn/Mn co-substitution plays a crucial role in altering the magnetic interactions between the cations. This redistribution leads to stronger magnetic interactions and, consequently, increased M_s and decreased coercivity in the co-substituted samples. The modified cation distribution within the spinel lattice is believed to influence the magnetic ordering and alignment of the magnetic moments, leading to the observed magnetic property changes. As the particle size of $Cu_{1-3x}Zn_{2x}Mn_xFe_2O_4$ samples increases, the microstructure becomes more ordered, resulting in fewer grain boundaries and defects. This reduced number of potential hindrances to magnetic domain alignment leads to improved saturation magnetization. The Néel model explains the total M_s of spinel ferrites, governed by the magnetization of both the A-site (M_A) and B-site (M_B) as following relation [39]:

$$M = M_B - M_A \quad (4)$$

An interesting observation was made regarding the magnetic properties of Zn/Mn co-substituted $CuFe_2O_4$ nanoparticles: as the level of Zn/Mn co-substitution increased, a significant decrease in magnetic anisotropy (M_A) occurred. This phenomenon is attributed to the presence of non-magnetic Zn^{2+} and Mn^{2+} ions occupying the tetrahedral sites within the spinel structure. As a result of this occupation, magnetic Fe^{3+} ions migrate to the octahedral sites, leading to a decrease in M_A. Simultaneously, the relocation of Fe^{3+} ions to the octahedral sites and the reduction of Cu^{2+} ions at these sites contribute to a substantial increase in magnetic moment (M_B).

Consequently, the overall effect of Zn/Mn co-substitution is an enhancement in the total saturation

magnetization of the samples, which aligns with predictions derived from the Néel model [40]. These findings emphasize the importance of cation distribution in determining the magnetic properties of spinel ferrites [41,42]. The redistribution of magnetic moments, in conjunction with the transition from hard to soft magnetic phases, demonstrates the potential of co-substitution as an effective method for fine-tuning the magnetic properties of these materials. This ability to modify magnetic characteristics opens up possibilities for tailoring spinel ferrites to meet specific application requirements [43-45], such as in magnetic storage devices, sensors, and energy conversion technologies. Zn/Mn co-substitution in $CuFe_2O_4$ nanoparticles leads to a decrease in magnetic anisotropy due to non-magnetic Zn^{2+}/Mn^{2+} ions occupying tetrahedral sites. This causes Fe^{3+} ions to migrate to octahedral sites, enhancing magnetic moment. The reduction of Cu^{2+} at these sites further increases saturation magnetization, consistent with the Néel model. Cation redistribution also promotes a transition from hard to soft magnetic behavior. These findings demonstrate the effectiveness of co-substitution in tuning the magnetic properties of spinel ferrites. In conclusion, the effects of Zn/Mn co-substitution on the magnetic properties of $CuFe_2O_4$ nanoparticles provide valuable insights into the underlying mechanisms governing their behavior. By manipulating the distribution of magnetic moments and controlling the transition between magnetic phases, researchers can harness the potential of these materials for various technological innovations, making co-substituted spinel ferrites a promising candidate for future applications in diverse fields.

4. Conclusions

A comprehensive study was conducted on a series of $Cu_{1-3x}Zn_{2x}Mn_xFe_2O_4$ samples synthesized using the citrate-nitrate method. The primary focus was to analyze the physical characteristics of these samples as a function of Zn/Mn co-substitution. XRD patterns obtained for the studied ferrites revealed an intriguing phase transition from tetragonal (space group $I4_1/amd$) to cubic (space group $Fd\bar{3}m$) as the level of Zn/Mn co-substitution increased. This observation was further corroborated by FTIR analysis, highlighting the role of co-substitution in modifying the crystal structure of $CuFe_2O_4$ spinel ferrites. Another notable finding was the decrease in the band gap of the $Cu_{1-3x}Zn_{2x}M_xFe_2O_4$ samples, ranging from 1.98 eV value for sample x=0.03 to 1.68 eV value for sample x=0.15, as the co-substitution level increased. This reduction in the band gap energy can be attributed to the alterations in the electronic structure and bonding characteristics of the nanoparticles, which could have implications for their optical and electronic properties. Magnetic measurements unveiled a transition from hard to soft magnetism with the Zn/Mn co-substitution. A significant decrease in H_c was observed for samples with higher co-substitution levels, indicating a lower energy barrier for magnetization reversal and an easier magnetization switching process. In contrast, the M_s of the studied samples displayed an upward trend, implying that the redistribution of Cu/Zn/Mn cations within the spinel lattice could enhance the exchange interactions between Fe^{3+} ions. The outcomes of this study underscore the role of the Zn/Mn co-doping in tailoring the properties of $CuFe_2O_4$ spinel ferrites. By manipulating the chemical composition and cation distribution, it is possible to fine-tune the physical properties of the studied ferrites, making them promising candidates for various applications such as magnetic materials, electronic devices, and energy storage systems.

Funding Statement

The Financial Support of the Research Council of Damghan University with Grant number 888077 is acknowledged.

Conflicts of interest

The authors declare that they have no known competing financial interests or personal relationships that could have appeared to influence the work reported in this paper.

Authors contribution statement

The Financial Support of the Research Council of Damghan University with Grant number 888077 is acknowledged.

References

[1] Liandi, A. R., Cahyana, A. H., Kusumah, A. J. F., Lupitasari, A., Alfariza, D. N., Nuraini, R., ... & Kusumasari, F. C. (2023). *Recent trends of spinel ferrites (MFe_2O_4: Mn, Co, Ni, Cu, Zn) applications as an environmentally friendly catalyst in multicomponent reactions: A review*. Case Studies in Chemical and Environmental Engineering, 7, 100303.

[2] Qin, H., He, Y., Xu, P., Huang, D., Wang, Z., Wang, H., ... & Wang, C. (2021). *Spinel ferrites (MFe_2O_4): Synthesis, improvement and catalytic application in environment and energy field.* Advances in Colloid and Interface Science, 294, 102486.

[3] Suresh, R., Rajendran, S., Kumar, P. S., Vo, D. V. N., & Cornejo-Ponce, L. (2021). *Recent advancements of spinel ferrite-based binary nanocomposite photocatalysts in wastewater treatment.* Chemosphere, 274, 129734.

[4] Satyanarayana, G., Rao, G. N., Babu, K. V., Kumar, G. S., & Reddy, G. D. (2020). *Influence of Chromium Substitution on Structural, Electrical, and Magnetic Properties of Ni–Zn–Cu Ferrites*. Acta Physica Polonica Series a 138(3):355-363.

[5] Kefeni, K. K., Msagati, T. A., Nkambule, T. T., & Mamba, B. B. (2020). *Spinel ferrite nanoparticles and nanocomposites for biomedical applications and their toxicity.* Materials Science and Engineering: C, *107*, 110314.

[6] Jacob, J., Javaid, K., Amin, N., Ali, A., Mahmood, K., Ikram, S., Arshad, M. I., Munir, A., & Amami, M. (2023). *The influence of lanthanum concentration on microstructural and electrical properties of Mg-Cd-Bi ferrite nanoparticles*, Ceramics International, 49(2), 1896-1901.

[7] Mojahed, M., Dizaji, H. R., & Gholizadeh, A. (2022). *Structural, magnetic, and dielectric properties of Ni/Zn co-*

substituted $CuFe_2O_4$ nanoparticles. Physica B: Condensed Matter, 646, 414337.

[8] Dastjerdi, O. D., Shokrollahi, H., & Mirshekari, S. (2023). *A review of synthesis, characterization, and magnetic properties of soft spinel ferrites.* Inorganic Chemistry Communications, 153, 110797.

[9] Gonçalves, J. M., de Faria, L. V., Nascimento, A. B., Germscheidt, R. L., Patra, S., Hernández-Saravia, L. P., ... & Angnes, L. (2022). *Sensing performances of spinel ferrites MFe_2O_4 (M= Mg, Ni, Co, Mn, Cu, and Zn) based electrochemical sensors: A review*. Analytica Chimica Acta, 1233, 340362.

[10] Salih, S. J., & Mahmood, W. M. (2023). *Review on magnetic spinel ferrite (MFe_2O_4) nanoparticles: From synthesis to application*. Heliyon, 9(6), e16601.

[11] Harrabi, D., Hcini, S., Dhahri, J., Wederni, M. A., Alshehri, A. H., Mallah, A., ... & Bouazizi, M. L. (2023). *Study of structural and optical properties of Cu–Cr substituted Mg–Co spinel ferrites for optoelectronic applications*. Journal of Inorganic and Organometallic Polymers and Materials, 33(1), 47-60.

[12] Kaur, S., Chalotra, V. K., Jasrotia, R., Bhasin, V., Kumari, S., Thakur, S., ... & Kumar Godara, S. (2022). *Spinel nano ferrite ($CoFe_2O_4$): The impact of Cr doping on its structural, surface morphology, magnetic, and antibacterial activity traits*. Optical Materials, 133, 113026.

[13] Peng, Y., Tang, H., Yao, B., Gao, X., Yang, X., & Zhou, Y. (2021). *Activation of peroxymonosulfate (PMS) by spinel ferrite and their composites in degradation of organic pollutants: A Review.* Chemical Engineering Journal, 414, 128800.

[14] Ferreira, L. S., Silva, T. R., Silva, V. D., Raimundo, R. A., Simões, T. A., Loureiro, F. J., ... & Macedo, D. A. (2022). *Spinel ferrite MFe_2O_4 (M= Ni, Co, or Cu) nanoparticles prepared by a proteic sol-gel route for oxygen evolution reaction*. Advanced Powder Technology, 33(1), 103391.

[15] Vinnik, D. A., Sherstyuk, D. P., Zhivulin, V. E., Zhivulin, D. E., Starikov, A. Y., Gudkova, S. A., ... & Trukhanov, A. V. (2022). *Impact of the Zn–Co content on structural and magnetic characteristics of the Ni spinel ferrites*. Ceramics International, 48(13), 18124-18133.

[16] Mahajan, H., Godara, S. K., & Srivastava, A. K. (2022). *Synthesis and investigation of structural, morphological, and magnetic properties of the manganese doped cobalt-zinc spinel ferrite*. Journal of Alloys and Compounds, 896, 162966.

[17] Murugesan, C., Ugendar, K., Okrasa, L., Shen, J., & Chandrasekaran, G. (2021). *Zinc substitution effect on the structural, spectroscopic, and electrical properties of nanocrystalline MnFe2O4 spinel ferrite*. Ceramics International, 47(2), 1672-1685.

[18] Sherstyuk, D. P., Starikov, A. Y., Zhivulin, V. E., Zherebtsov, D. A., Gudkova, S. A., Perov, N. S., ... & Trukhanov, A. V. (2021). *Effect of Co content on magnetic features and SPIN states IN Ni–Zn spinel ferrites*. Ceramics International, 47(9), 12163-12169.

[19] Nasr, M. H., Elkholy, M. M., El-Deen, L. M. S., Turky, G. M., Moustafa, M., EL-Hamalawy, A. A., & Abouhaswa, A. S. (2024). Synthesis, structural, electrical and magnetic characteristics of Co–Cd spinel nano ferrites synthesized via sol-gel auto combustion method. *Journal of Sol-Gel Science and Technology*, 1-13.

[20] Dojcinovic, M. P., Vasiljevic, Z. Z., Pavlovic, V. P., Barisic, D., Pajic, D., Tadic, N. B., & Nikolic, M. V. (2021). *Mixed Mg–Co spinel ferrites: Structure, morphology, magnetic and photocatalytic properties*. Journal of alloys and compounds, 855, 157429.

[21] Patil, R. P., Elhouichet, H., Iqbal, M., & Ayyar, M. (2025). Highly stable dielectric frequency response of chemically synthesized Cobalt substituted Zn-Mn-Ferrites. *Ceramics International*.

[22] Abd-Elbaky, H. G., Rasly, M., Deghadi, R. G., Mohamed, G. G., & Rashad, M. M. (2022). Strong-base free synthesis enhancing the structural, magnetic and optical properties of Mn/Co and Zn/Co substituted cobalt ferrites. *Journal of Materials Research and Technology*, *20*, 905-915.

[23] Ghodake, U. R., Chaudhari, N. D., Kambale, R. C., Patil, J. Y., & Suryavanshi, S. S. (2016). Effect of Mn^{2+} substitution on structural, magnetic, electric and dielectric properties of Mg–Zn ferrites. *Journal of Magnetism and Magnetic Materials*, *407*, 60-68.

[24] Mazen, S., Abu-Elsaad, N. I., & Nawara, A. S. (2020). The Influence of Various Divalent Metal Ions (Mn^{2+}, Co^{2+}, and Cu^{2+}) Substitution on the Structural and Magnetic Properties of Nickel–Zinc Spinel Ferrite. *Physics of the Solid State*, *62*, 1183-1194.

[25] Eghdami, F., & Gholizadeh, A. (2023). A correlation between microstructural and impedance properties of MnFe2-xCoxO4 nanoparticles. *Physica B: Condensed Matter*, *650*, 414551.

[26] Sefatgol, R., & Gholizadeh, A. (2022). The effect of the annealing temperature on the microstructural, magnetic, and spin-dynamical properties of Mn–Mg–Cu–Zn ferrites. *Physica B: Condensed Matter*, *624*, 413442.

[27] El-Masry, M. M., & Ramadan, R. (2022). The effect of $CoFe_2O_4$, $CuFe_2O_4$ and $Cu/CoFe_2O_4$ nanoparticles on the optical properties and piezoelectric response of the PVDF polymer. *Applied Physics A*, *128*(2), 110.

[28] Takalloo, F., Gholizadeh, A., & Ardyanian, M. (2024). Crystal structure-physical properties correlation in Ni–Cu–Zn spinel ferrite. *Journal of Materials Science: Materials in Electronics*, *35*(27), 1792.

[29] Choupani, M., & Gholizadeh, A. (2024). Correlation between structural phase transition and physical properties of Co^{2+}/Gd^{3+} co-substituted copper ferrite. *Journal of Rare Earths*, *42*(7), 1344-1353.

[30] Kazemi, N., & Mahdavi Shahri, M. (2017). Magnetically separable and reusable $CuFe_2O_4$ spinel nanocatalyst for the O-arylation of phenol with aryl halide under ligand-free condition. *Journal of Inorganic and Organometallic Polymers and Materials*, *27*, 1264-1273.

[31] Shamgani, N., & Gholizadeh, A. (2019). Structural, magnetic and elastic properties of $Mn_{0.3-x}Mg_xCu_{0.2}Zn_{0.5}Fe_3O_4$ nanoparticles. *Ceramics International*, *45*(1), 239-246.

[32] Gholizadeh, A., & Beyranvand, M. (2020). Investigation on the structural, magnetic, dielectric and impedance analysis of $Mg_{0.3-x}Ba_xCu_{0.2}Zn_{0.5}Fe_2O_4$ nanoparticles. *Physica B: Condensed Matter*, *584*, 412079.

[33] Sefatgol, R., Gholizadeh, A., & Hatefi, H. (2024). Effect of Ti Substitution on the Structural, Optical, and Magnetic Properties of Mn-Mg-Cu-Zn Ferrite Prepared by the Sol–Gel Route. *Journal of Electronic Materials*, *53*(10), 6140-6150.

[34] Shannon, R. T., & Prewitt, C. T. (1969). Effective ionic radii in oxides and fluorides. *Structural Science*, *25*(5), 925-946.
[35] Voorhees, P. W. (1985). The theory of Ostwald ripening. *Journal of Statistical Physics*, *38*, 231-252.
[36] Khedr, A., & Striolo, A. (2019). Quantification of Ostwald ripening in emulsions via coarse-grained simulations. *Journal of chemical theory and computation*, *15*(9), 5058-5068.
[37] López, R., & Gómez, R. (2012). Band-gap energy estimation from diffuse reflectance measurements on sol–gel and commercial TiO_2: a comparative study. *Journal of sol-gel science and technology*, *61*, 1-7.
[38] Makuła, P., Pacia, M., & Macyk, W. (2018). How to correctly determine the band gap energy of modified semiconductor photocatalysts based on UV–Vis spectra. *The journal of physical chemistry letters*, *9*(23), 6814-6817.
[39] Mojahed, M., Gholizadeh, A., & Dizaji, H. R. (2024). Influence of Ti^{4+} substitution on the structural, magnetic, and dielectric properties of Ni-Cu–Zn ferrite. *Journal of Materials Science: Materials in Electronics*, *35*(18), 1239.
[40] Spaldin, N. A. (2010). *Magnetic materials: fundamentals and applications*. Cambridge university press.
[41] Beyranvand, M., & Gholizadeh, A. (2020). Structural, magnetic, elastic, and dielectric properties of $Mn_{0.3-x}Cd_xCu_{0.2}Zn_{0.5}Fe_2O_4$ nanoparticles. *Journal of Materials Science: Materials in Electronics*, *31*(7), 5124-5140.
[42] Gholizadeh, A., & Jafari, E. (2017). Effects of sintering atmosphere and temperature on structural and magnetic properties of Ni-Cu-Zn ferrite nano-particles: Magnetic enhancement by a reducing atmosphere. *Journal of Magnetism and Magnetic Materials*, *422*, 328-336.
[43] Hakeem, A., Alshahrani, T., Muhammad, G., Alhossainy, M. H., Laref, A., Khan, A. R., ... & Khosa, R. Y. (2021). Magnetic, dielectric and structural properties of spinel ferrites synthesized by sol-gel method. *Journal of Materials Research and Technology*, *11*, 158-169.
[44] Butt, K. Y., Aman, S., AlObaid, A. A., Al-Muhimeed, T. I., Rehman, A., Hegazy, H. H., ... & Farid, H. M. T. (2021). The study of structural, magnetic and dielectric properties of spinel ferrites for microwave absorption applications. *Applied Physics A*, *127*(9), 714.
[45] Yang, H., Yang, X., Lin, J., Yang, F., He, Y., & Lin, Q. (2023). Effect of Cd^{2+} substitution on structural–magnetic and dielectric properties of Ni–Cu–Zn spinel ferrite nanomaterials by Sol–Gel. *Molecules*, *28*(16), 6110.